PAPER

Check for updates

First principle study and Hirshfeld surface analysis on the effect of type, number, and position of small molecules on the structural stability and optical property of a powerful energetic crystal 6-nitro-7-azido-pyrazol[3,4-*d*][1,2,3]triazine-2-oxide

Qiong Wu, [ID] *[abc] Tao Sun,[a] Linghua Tan[bc] and Weihua Zhu [ID] [c]

In the present study, the detailed functions of three small molecules, H_2O, NH_3, and H_2S, on the structural stability of a novel high energy compound 6-nitro-7-azido-pyrazol[3,4-*d*][1,2,3]triazine-2-oxide (ICM-103) with high application value were investigated by the first principle study and Hirshfeld surface analysis. The effects of type, number, and position of small molecules on the molecular, crystal and electronic structures, close contacts and sensitivity, and optical properties of ICM-103 were also studied. First, the relatively high sensitivity feature used as initiating explosives of ICM-103 was confirmed, but H_2O, NH_3, and H_2S all could stabilize the structure of ICM-103 to reduce sensitivity by enhancing close contacts such as hydrogen bonding and increasing the ratio of red dots located on the block edge of Hirshfeld surface. This function could be further improved with the increment of number, and small molecules in two different positions were found to have a synergistic effect on stabilizing the structure. The stabilization ability of NH_3 was found to be stronger than H_2O and H_2S due to the highest stabilization energy and strongest close contacts. Then, H_2O and NH_3 reduced the absorption intensity to ultraviolet light but enhanced the absorption to visible light and infrared light. Three molecules all increased the dielectric constant and static refractive index with the order of H_2S, and H_2O, NH_3. NH_3 eliminated the region, in which light could not be transmitted in other crystals. Finally, the position of NH_3 was found to have significant effects on the structure and properties of ICM-103, while this is not obvious for H_2O and H_2S.

1. Introduction

The energetic compound is one kind of active, special but very important energy material that releases huge power in an extremely short time when stimulated by external energy factors including impact, heat, friction, and electricity. Thus, it can be applied in many fields including national defence, aerospace and tunneling, in which it may be used as a high explosive, gun, solid rocket propellant, primary explosive, *etc.* Among different kinds of energetic compounds, the high energy density compound has attracted lot of attention from researchers due to its outstanding performance such as high detonation properties. Lately, some good representatives including all-nitrogen pentazole series (N_5),[1–7] ICM series,[8–10] and high energy cage compounds[11] have been designed and synthesized successfully. However, due to their high energy, many of them have low stability and high sensitivity. However, at the same time, an interesting phenomenon was observed in which a different number of small molecules such as H_2O (or H_3O^+) and NH_3 (or NH_4^+) coexisted with energetic molecules in the crystal. For example, these reported pentazole energetic compounds include $[M(H_2O)_4(N_5)_2] \cdot 4H_2O$ (M = Mn, Fe, Co, Zn)[1] and $(N_5)_6(H_3O)_3(NH_4)_4Cl$.[2] For the ICM series, in the crystal of an insensitive compound 2,4,6-triamino-5-nitropyrimidine-1,3-dioxide (ICM-102),[9] or in the crystal of a fused-ring initiating substance 6-nitro-7-azido-pyrazol[3,4-*d*][1,2,3]triazine-2-oxide (ICM-103),[10] a different number of H_2O were observed. For the high energy cage compound, H_2O was also found in the crystal of one of the most powerful compounds 2,4,6,8,10,12-hexanitro-2,4,6,8,10,12-hexaazatetracyclo[5.5.0.0.0] dodecane (CL-20).[11] Thus, it is necessary to clearly learn and

[a] *School of Materials Science and Engineering, Jiangsu Key Laboratory of Advanced Structural Materials and Application Technology, Nanjing Institute of Technology, Nanjing 211167, China. E-mail: qwunjit@163.com*

[b] *National Special Superfine Powder Engineering Research Center, Nanjing 210014, China*

[c] *Nanjing University of Science and Technology, Nanjing 210094, China*

understand the reason for these small molecules coexisting with energetic molecules in the crystal as well as their functions and effects on the structures and properties of different energetic crystals. Based on the quantum mechanical calculation, Luo[12] has found that two kinds of H_2O are in the $[M(H_2O)_4(N_5)_2]\cdot 4H_2O$ (M = Mn, Fe, Co, Zn) system, and they can participate in both the coordination and hydrogen bonding to stabilize the whole structure. In addition, the hot H_2O was found that can catalyze the decomposition of pentaerythritol tetranitrate[13] and furoxan[14] by transporting oxygen between reaction centers under extremely high temperature/pressure, and the content of H_2O was found to affect the thermal decomposition of ammonium dinitramide.[15] Our previous work[16] found that the H_2O can stabilize the crystal structure and reduce the impact insensitivity of ICM-102 by enhancing the hydrogen bonding and other intermolecular interactions. H_2O will also improve the density, mechanical performance, and thermodynamics parameters of ICM-102. In all, since energetic compounds are dangerous materials and sensitive to the internal/external environment, these above mentioned studies may show the effects of small molecules on the structure and property under different conditions. Thus, in order to increase the safety in operation, processing and usage, enhance the application value, and guide the design of new advanced energetic compounds, it is important and necessary to investigate and understand these clearly and deeply.

ICM-103 (as seen in Fig. 1) is a new synthetic high energy compound,[10] whose heat of formation (744.8 kJ mol^{-1}), heat of combustion (739.4 kJ mol^{-1}), density (1.86 g cm^{-3}), detonation velocity (D = 9.1 km s^{-1}), and detonation pressure (P = 35.1 GPa) are apparently higher than 2-diazo-4,6-dinitrophenol (D = 6.9 km s^{-1})[17] and lead azide (D = 5.9 km s^{-1}),[18] showing its outstanding detonation performance. While its impact sensitivity, friction sensitivity, and electrostatic discharge sensitivity are 4 J, 60 N, and 130 mJ, respectively, which are also obviously superior to those of 2-diazo-4,6-dinitrophenol (1 J, 24.7 N, and 1.8 mJ)[17] and lead azide (2.5–4 J, 0.1–1 N, and <5 mJ).[18] The excellent combination performance of ICM-103 shows its tremendous application foreground as an initiating explosive device to replace 2-diazo-4,6-dinitrophenol and lead azide. As an initiating explosive, ICM-103 is even more sensitive to various structural and environmental factors than secondary explosives like CL-20 and insensitive compounds like ICM-102, and clearly understanding its structure and property will be essential to accelerate the application. From the crystal structure,

two kinds of H_2O molecules at two different positions (positions 1 and 2) were found (as seen in Fig. 1b), and each one has two H_2O molecules. Thus, in the present work, using the first principle calculation and Hirshfeld surface analysis method, the molecular, crystal and electronic structures, the safe and optical properties of ICM-103 were studied. Effects of three kinds of small molecules (H_2O, NH_3, and H_2S) with a different number (0, 2, and 4) at two different positions on the structure and properties were investigated and explored comprehensively.

2. Computational methods

First of all, all first-principle calculations on the ICM-103 crystal were performed using the CASTEP module.[19] The norm-conserving pseudopotential,[20] GGA-PW91 with the OBS correction (labeled as GGA-PW91-OBS),[21] and the BFGS[22] optimization method were used. The cutoff (750 eV), k-point (3 × 5 × 1), and SCF tolerances (fine grade) were set. There are four H_2O molecules in the crystal of ICM-103, two H_2O are in position 1 while the other two are in position 2, as seen in Fig. 1b. The original experimental crystal structure[10] of ICM-103 (labeled as ICM-103-4H_2O) was used as the input structure and relaxed. Then, based on this relaxed structure, all four H_2O, two H_2O in positions 1 and 2 were deleted to form the ICM-103-0H_2O and the other two H_2O-crystals (ICM-103-2H_2O-1 and ICM-103-2H_2O-2), respectively. All four H_2O, two H_2O in positions 1 and 2, were replaced by a corresponding number of NH_3 and H_2S to form three NH_3-crystals (ICM-103-4NH_3, ICM-103-2NH_3-1, ICM-103-2NH_3-2) and three H_2S crystals (ICM-103-4H_2S, ICM-103-2H_2S-1, and ICM-103-2H_2S-2), respectively. Since H_2O, NH_3, and H_2S can act as both the donor and acceptor of hydrogen bonds, their size and function are similar to each other. Thus, it may be supposed that they will occupy similar initial lattice sites in the crystal structure of ICM-103. These 9 newly formed crystals were then relaxed using the same method and set as ICM-103-4H_2O to obtain their corresponding stable crystals. The small molecules were allowed to diffuse freely during the relaxation simulation. Based on the relaxed crystals, the band structure, band gap, density of states (DOS), and optical properties were calculated and estimated. The optimization and energy calculations of single H_2O, NH_3, and H_2S were performed in a big periodic cell, which has the same scale as the corresponding ICM-103 crystal. The stabilization energy (ΔE) was predicted by the following equation: $\Delta E = E_{cry} - (n \times E_{sm} + E_{NW})$. E_{cry} means the energy of ten crystals, n is the amount of the corresponding small molecules, E_{sm} is the energy of the corresponding single small molecule, and E_{NW} represents the energy of crystal ICM-103-0H_2O. Finally, the Hirshfeld surface analysis calculations of ten ICM-103 crystals were performed using the CrystalExplorer 3.0 program.[23]

3. Results and discussion

3.1. Crystal structure

The GGA-PW91-OBS method was used to relax and optimize the crystal structure of ICM-103-4H_2O at ambient conditions
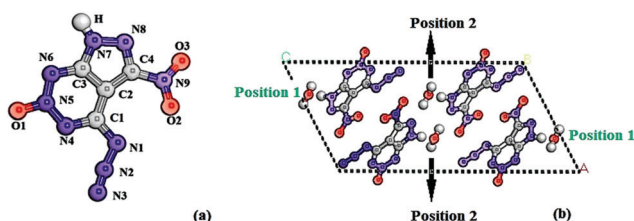

Fig. 1 The single molecule structure and atomic number (a) and crystal structure (b) of ICM-103.

without any constraint, and the predicted lattice constants are listed in Table 1. It can be found that the calculated values are close to the experimental results, and the errors ranged from 0.7% to 3.8%. A comparison of the bond length of main chemical bonds between the theoretical and experimental results has been made, and the errors are very small, as seen in Table 2. The above results show the high accuracy of the used method. Thus, the GGA-PW91-OBS method was also used to relax other newly formed crystals, and the results have been listed in Table 1. It is found that the lattice parameters are sensitive to the type, number, and position of three small molecules. First of all, since three small molecules will occupy the space in crystals, the volume (V) enlarges with the increased number of small molecules in each series. Then, the length of the S–H bond is obviously larger than those of the N–H and O–H bonds, thus, leading to a larger volume and lower density apparently for H_2S-crystals. As density is an important parameter related to the energy performance of energetic crystals and for energetic compounds with similar structures, the lower the density is, the lower the energy. Therefore, H_2S may be less helpful for obtaining higher energy compared with the other two small molecules. Finally, due to the fact that small molecules are mainly occupied in the space along the b and c directions, the crystals within small molecules all have longer b and c than crystals without small molecules or within fewer small molecules. As a result, generally, H_2S-crystals have longer a, c, and volume than NH_3-crystals than H_2O-crystals, while this is just the opposite for b.

The bond length of various bonds in ICM-130 molecules was found to be also affected by small molecules. For the ICM-103 molecule, the NO_2 and N_3 groups may be the most sensitive sites to stimulus and have the main effects on sensitivity and safety. The C–NO_2 bond is easy to break, while the C1N1–N2N3 bond (as seen in Fig. 1) in the N_3 group is also easy to break to release N_2 gas. Thus, the effects of small molecules on the bond length of these two bonds (C–NO_2 and N1–N2 bonds) were studied and are listed in Table 3. It is found that ICM-103-$4H_2O$, ICM-103-$2H_2O$-1, and ICM-103-$2H_2O$-2 have shorter C–NO_2 bonds than ICM-103-$0H_2O$, especially for ICM-103-$4H_2O$, whose two C–NO_2 bonds are both 0.6% shorter than ICM-103-$0H_2O$. This is even more obvious for NH_3-crystals, with

Table 2 A comparison of the bond length of main chemical bonds between the theoretical and experimental results for ICM-103-$4H_2O$

Bond	Expt. (Å)	GGA-PW91-OBS (Å)	Absolute error (Å)	Relative error (%)
N1–N2	1.291	1.287	0.004	0.3
C1–N1	1.372	1.392	0.02	1.5
C1–N4	1.346	1.348	0.002	0.1
C1–C2	1.403	1.411	0.008	0.6
N5–N4	1.346	1.375	0.029	2.2
N5–O1	1.253	1.265	0.012	1.0
N5–N6	1.308	1.349	0.041	3.1
N6–C3	1.352	1.348	0.004	0.3
C3–C2	1.393	1.414	0.021	1.5
C3–N7	1.338	1.363	0.025	1.9
N7–N8	1.352	1.366	0.014	1.0
N8–C4	1.313	1.339	0.026	2.0
C4–C2	1.399	1.418	0.019	1.4
C4–N9	1.447	1.450	0.003	0.2
N9–O3	1.222	1.241	0.019	1.6
N9–O2	1.214	1.242	0.028	2.3

the two C–NO_2 bonds of ICM-103-$4NH_3$ being about 1.7% shorter than those of ICM-103-$0H_2O$. This is because the small molecules in the crystal of ICM-103 will help generate the hydrogen bonds between NO_2 and small molecules, which increases the stability of NO_2 groups and leads to stronger and shorter C–NO_2 bonds. The N1–N2 bonds of NH_3-crystals are also about 0.4–1.1% shorter than ICM-103-$0H_2O$. For the three H_2S-crystals, their C-NO_2 and N1–N2 bonds are slightly shorter than ICM-103-$0H_2O$ in general. In each series, the crystals with four small molecules have the shortest C–NO_2 and N1–N2 bonds. Fig. 2 displays the optimized structures of 9 newly formed crystals. It is found the relative positions of energetic molecules and small molecules in H_2O-crystals and H_2S-crystals are not changed obviously compared to ICM-103-$4H_2O$. But it is interesting to find the H atom linked with N7 in ICM-103 molecules has transferred from ICM-103 to the N atom in NH_3 to form NH_4, which is different from that of H_2O and H_2S. This may suggest that NH_3-crystals may transform from neutral to ionic type energetic compounds, as NH_3 usually tends to exist in the form of NH_4 when contained in energetic crystals. Many NH_4-related energetic compounds like ammonium dinitramide (ADN), ammonium perchlorate (AP), and $(N_5)_6(H_3O)_3(NH_4)_4Cl$ have been synthesized and reported before.

Table 1 Relaxed lattice parameters of all ten ICM-103 crystals with the experimental data at ambient conditions

Parameter	a (Å)	b (Å)	c (Å)	β (°)	V (Å³)
ICM-103-$4H_2O$/Expt.	9.931	5.210	19.767	116.4	916.0
ICM-103-$4H_2O$/GGA-PW91-OBS	10.038 $(1.1\%)^a$	5.409 $(3.8\%)^a$	19.611 $(0.7\%)^a$	117.7 $(1.1\%)^a$	943.1 $(3.0\%)^a$
ICM-103-$0H_2O$	10.414	5.107	19.486	117.3	921.0
ICM-103-$2H_2O$-1	10.146	5.296	19.624	117.2	937.3
ICM-103-$2H_2O$-2	10.104	5.324	19.547	117.1	934.9
ICM-103-$4NH_3$	10.464	5.075	22.178	123.7	979.8
ICM-103-$2NH_3$-1	10.122	5.282	21.321	124.4	931.4
ICM-103-$2NH_3$-2	10.309	5.127	20.275	118.3	943.2
ICM-103-$4H_2S$	10.855	5.082	22.529	119.2	1085.0
ICM-103-$2H_2S$-1	10.688	5.000	21.794	118.3	1025.2
ICM-103-$2H_2S$-2	10.668	5.003	21.741	118.2	1022.4

^{a} The absolute values in parentheses correspond to the percentage differences relative to the experimental data.

Table 3 The bond lengths (Å) of C–NO$_2$ and N1–N2 bonds, stabilization energy (ΔE, eV), band gap (GAP, eV), dielectric constant [$\varepsilon_1(0)$], and refractive indices (n_0) of ten ICM-103 crystals

Crystal	C–NO$_2$		N1–N2		ΔE	GAP	$\varepsilon_1(0)$	n_0
ICM-103-0H$_2$O	1.459	1.459	1.288	1.288	0	2.287	1.941	1.393
ICM-103-4H$_2$O	1.450	1.450	1.287	1.287	−5.01	2.217	2.047	1.431
ICM-103-2H$_2$O-1	1.459	1.450	1.291	1.291	−2.36	2.182	1.950	1.396
ICM-103-2H$_2$O-2	1.459	1.450	1.289	1.284	−2.38	2.182	1.950	1.396
ICM-103-4NH$_3$	1.434	1.434	1.274	1.274	−7.56	2.133	2.039	1.428
ICM-103-2NH$_3$-1	1.460	1.427	1.280	1.279	−3.74	1.595	2.062	1.436
ICM-103-2NH$_3$-2	1.459	1.437	1.283	1.280	−3.37	1.955	2.126	1.458
ICM-103-4H$_2$S	1.458	1.458	1.286	1.286	−2.38	2.059	2.011	1.418
ICM-103-2H$_2$S-1	1.459	1.456	1.289	1.282	−1.03	2.040	1.979	1.407
ICM-103-2H$_2$S-2	1.459	1.459	1.289	1.282	−1.03	2.040	1.979	1.407

3.2. Electronic structure

The small molecules were found to influence the electronic structure of ICM-103 crystals. First, the estimated band gap values of ten crystals have been listed in Table 3. It is found that ICM-103-0H$_2$O has the highest band gap, showing that the electron transfer from the valence band to the conduction band is more difficult than in other crystals. Since three small molecules have different effects on the crystal and molecular structures, the band gap is changed to different degrees. For example, the band gap decreases with the order of ICM-103-0H$_2$O, H$_2$O-crystals, and H$_2$S-crystals in general. The energy levels in band structures for H$_2$O and H$_2$S molecules are located between 0−−20 eV rather than between the HOMO and LUMO of ICM-103. Thus, the band gap values of H$_2$O-crystals and H$_2$S-crystals have not reduced obviously and are close to ICM-103-0H$_2$O. But for NH$_3$-crystals, due to the change from neutral to ionic crystals and forming of NH$_4$, the electronic structures have been affected more obviously compared to others. As a result, their band gap values are different from each other and all lower than ICM-103-0H$_2$O. The band gap of ICM-103-2H$_2$O-1/2 and ICM-103-2H$_2$S-1/2 are the same, respectively. But the

band gap of ICM-103-2NH$_3$-1 is obviously lower than that of ICM-103-2NH$_3$-2, showing that the effects of the position and type of small molecules on the band gap coupled with each other. The band gap values of ICM-103 crystals are generally small, showing that the electron-related chemical reaction is easy to occur and is in agreement with the feature of initiating explosives.

Fig. 3 displays the band structures of ten ICM-103 crystals. When compared with ICM-103-0H$_2$O, it is observed from Fig. 3a that ICM-103-4H$_2$O, ICM-103-4NH$_3$, and ICM-103-4H$_2$S all have more energy levels due to the contribution and effect of the corresponding small molecules. But the effects of small molecules on the energy levels at the valence band and conduction band are different. H$_2$O and NH$_3$ will induce the energy level at the valence band and conduction band to red-shift and blue-shift, respectively, while H$_2$S will induce some of the energy levels at the valence band to blue-shift. The number of H$_2$O and H$_2$S also affects the band structure to some degree, but their positions have negligible influence, as seen in Fig. 3b and d. The position and number of NH$_3$ both have significant effects on the band structure. The energy levels in ICM-103-2NH$_3$-1 are lower than those in ICM-103-2NH$_3$-2 and ICM-103-4NH$_3$, especially at the conduction band, as seen in Fig. 3c.

Finally, Fig. 4 further depicts the DOS of ten ICM-103 crystals. From Fig. 4a, it can be seen that H$_2$O, NH$_3$, and H$_2$S all make contributions to different DOS peaks. For H$_2$O, it makes contributions to peaks at energies of −19 eV and −8–0 eV. For NH$_3$, its contributions occur at energies −17 and −8–−5 eV. H$_2$S makes significant contributions to peaks around Fermi level (−3–0 eV) and two other peaks at −16 eV and −8.5 eV, which may be because ICM-103-4H$_2$S has more energy levels than ICM-103-0H$_2$O at 0–3 eV. As a result, ICM-103-4H$_2$O, ICM-103-4NH$_3$, and ICM-103-4H$_2$S have different DOS compared to ICM-103-0H$_2$O. The effects of the number on DOS are mainly on the peak intensity, while the position of small molecules on DOS is not
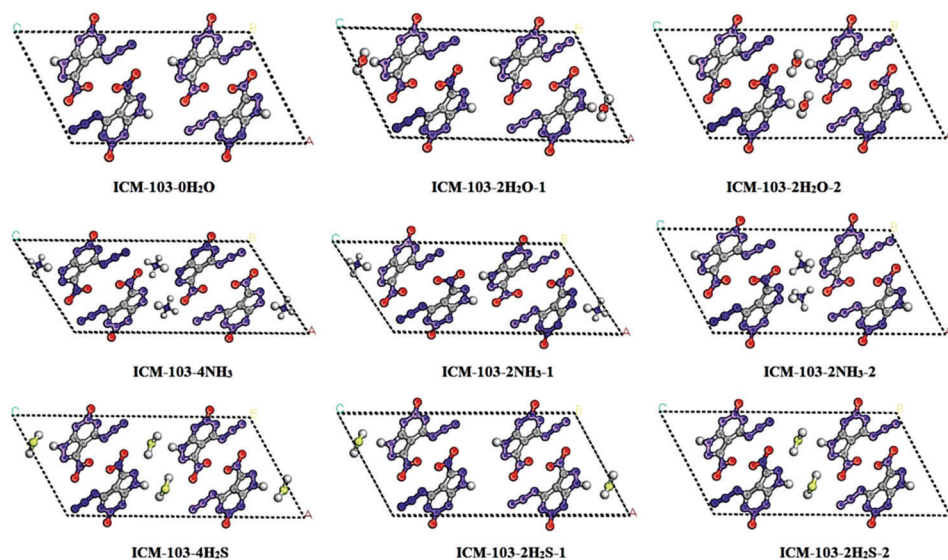

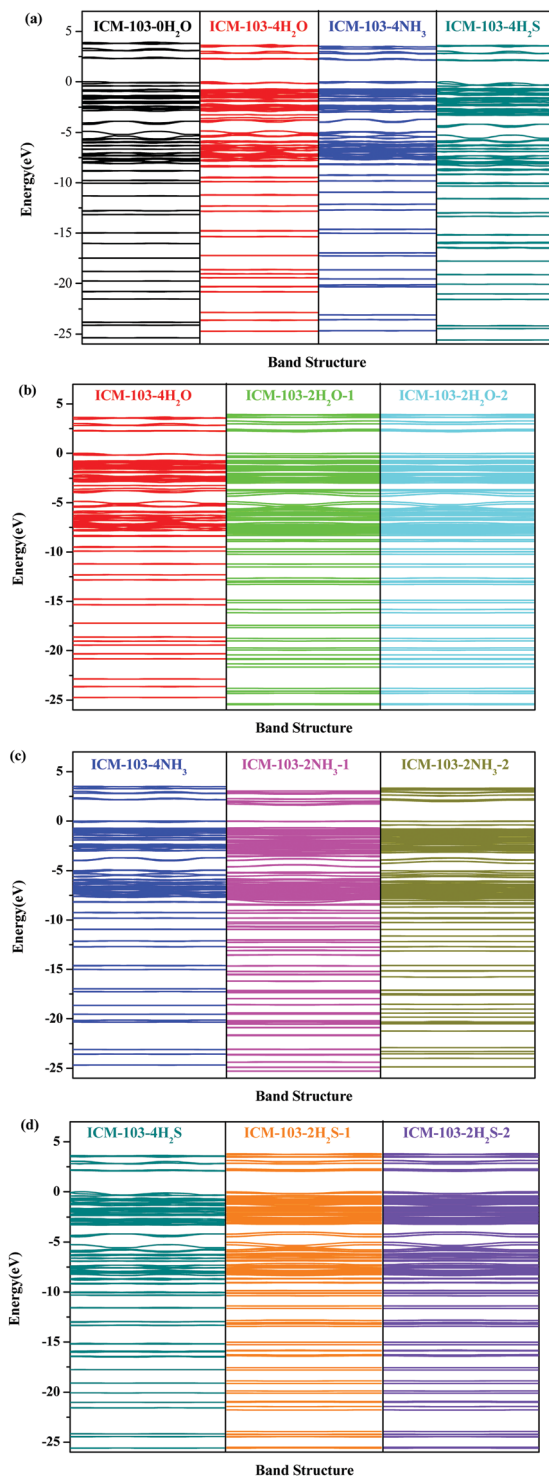**Fig. 2** The optimized crystal structures of nine newly formed ICM-103 crystals.

© 2022 The Author(s). Published by the Royal Society of Chemistry

Fig. 3 A comparison of the band structure of ten ICM-103 crystals.

Fig. 4 A comparison of the DOS of ten ICM-103 crystals.

obvious, as seen in Fig. 4b–d. In all, it is found that the type, number, and position of small molecules indeed can influence the molecular, crystal, and electronic structures of ICM-103. These effects are different from each other and may be coupled with each other sometimes, which may indicate that they will also affect the properties of ICM-103.
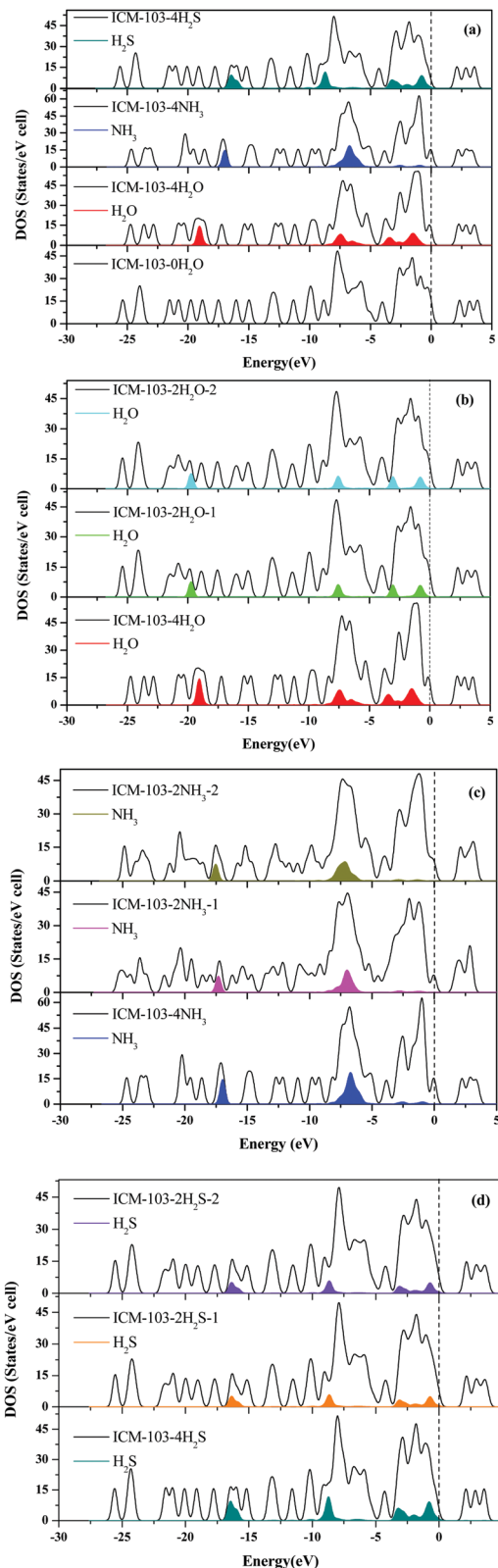
3.3. Hirshfeld surface

Hirshfeld surface[16,24–26] can provide a lot of useful information for understanding the intermolecular contacts and impact the
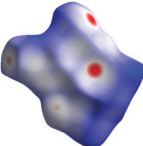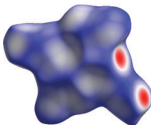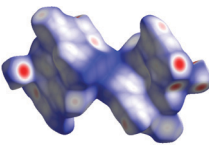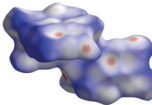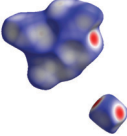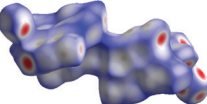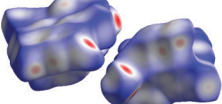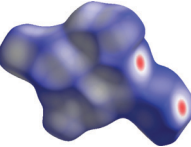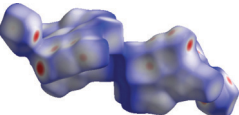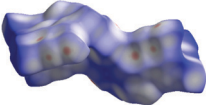
sensitivity of energetic crystals. Table 4 lists the predicted d_{norm} mapped on Hirshfeld surface (HS) for visualizing intermolecular and ratio of red dots located on the block edge ($E\%$) of ten ICM-103 crystals. Generally, it is observed that all other 9 crystals have more red spot areas than ICM-103-0H$_2$O, showing that H$_2$O, NH$_3$, and H$_2$S can strengthen close contacts in ICM-103 crystals obviously, and this may be helpful for increasing the close contact intensity and stabilizing the system. Then, it has been reported that when more red dots are located on the block edge, the impact sensitivity of energetic compounds will be lower. As seen in Table 4, the $E\%$ value of ICM-103-0H$_2$O is 50%, showing that half of the red hot dots are not located on the edge area, and ICM-103 is a relatively sensitive energetic compound, which conforms to its characteristic as an initiating explosive. However, this can be improved to some degree, as found for all other 9 crystals, with higher $E\%$ than ICM-103-0H$_2$O, especially for the crystals containing four small molecules, whose $E\%$ values are higher than 80%. This indicates that H$_2$O, NH$_3$, and H$_2$S in the ICM-103 system may be good for decreasing the impact sensitivity, and this positive effect will be more obvious with the increment of the number of molecules. The effects of the position of small molecules on the $E\%$ are not obvious.

For a deeper understanding of the detailed close intermolecular contacts in different ICM-103 crystals, Fig. 5 displays the fingerprint plots of contacts of ten crystals. Generally, a smaller d_i (the distances from the surface to the nearest atom inside the surface) + d_e (the distances from the surface to the nearest atom outside the surface) will lead to a closer atom–atom contact, and the contact being stronger and stronger

when the color changes from blue to blue-green and green. Therefore, from Fig. 5, it can be seen that the contribution to the whole picture within lower d_i (2.0 Å) + d_e (2.0 Å) in all 9 small molecule-containing crystals is much larger than in ICM-103-0H$_2$O, and the green and blue-green regions are also wider than ICM-103-0H$_2$O, showing that all three small molecules H$_2$O, NH$_3$ and H$_2$S can increase close contacts in ICM-103 crystals apparently. Then, it is found that this decreases with the order of NH$_3$-crystals, H$_2$O-crystals, and H$_2$S-crystals, indicating that NH$_3$ is the most favourable molecule for enhancing the close contacts and may also be true for stabilizing the system. One main reason is that the small molecules can increase the intermolecular hydrogen-bonding contact (N/O/S⋯H), as seen from Fig. 6. It can be found that the O⋯N, N⋯N, and N/O/S⋯H are three main contacts in each crystal, but their percentage values are different. In ICM-103-0H$_2$O, the percentage of O⋯N contact is the highest among all close contacts, but this is N/O/S⋯H for other small molecule containing crystals, in which the percentage of the N/O/S⋯H increases in the order of ICM-103-0H$_2$O (20.6%), ICM-103-4H$_2$S (31.8%), ICM-103-4H$_2$O (32.2%), and ICM-103-4NH$_3$ (46%), leading to the stronger hydrogen bonding and better stabilizing function on the crystal structure. More information is further supported by Fig. 7, in which it can be clearly seen that the number of intermolecular contact network lines and strength of N/O/S⋯H contacts also increase in the same order as mentioned above. However, this is different from that of ICM-102 crystal,[16] in which the H$_2$O is the most favourable one to stabilize the system, showing that

Table 4 The d_{norm} mapped on Hirshfeld surface (HS) for visualizing intermolecular and ratio of red dots located on the block edge ($E\%$) of ten ICM-103 crystals

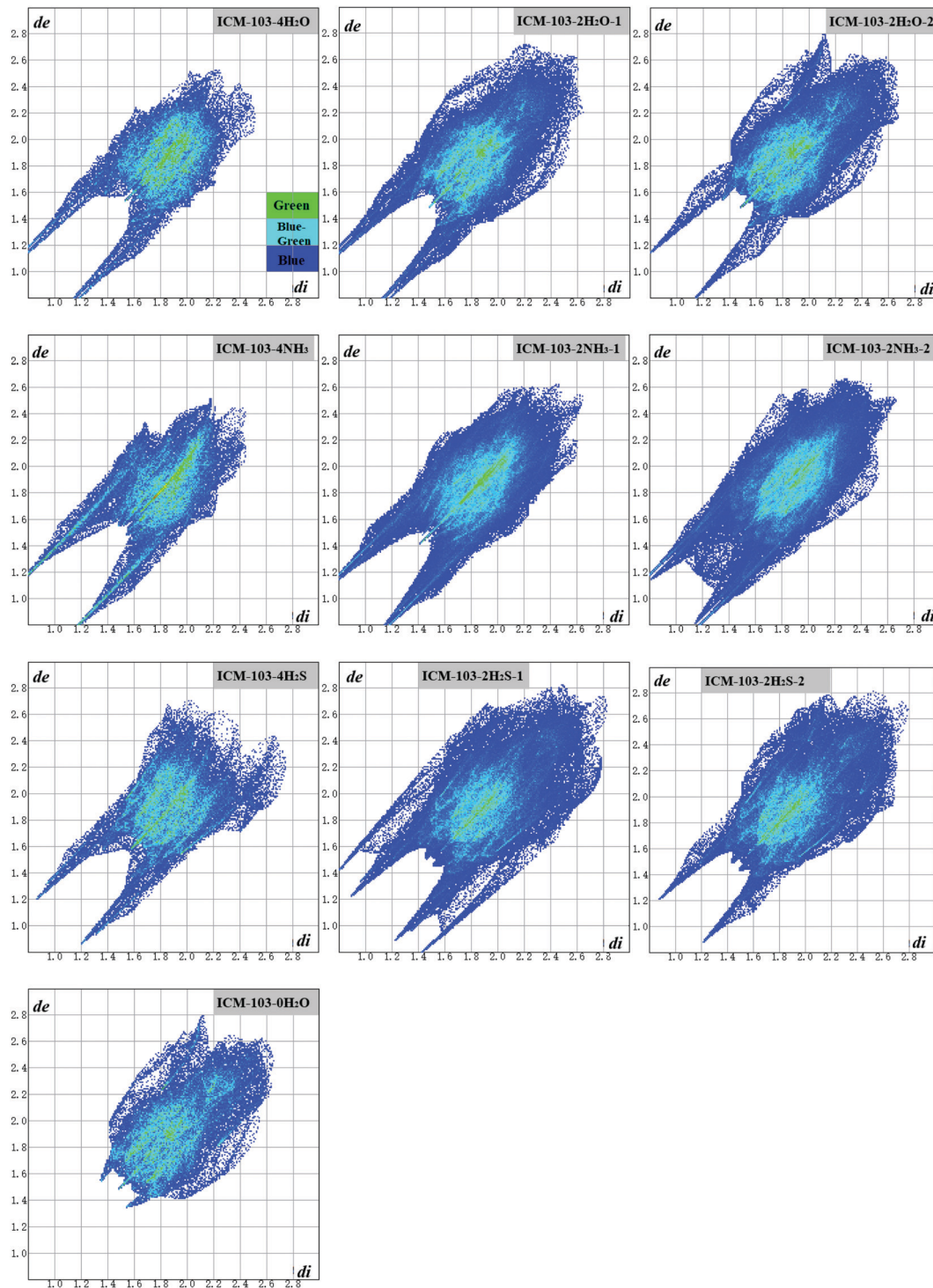|	ICM-103-0H$_2$O	ICM-103-4H$_2$O	ICM-103-2H$_2$O-1	ICM-103-2H$_2$O-2
HS				
$E\%$	50	86	54	56
	ICM-103-4NH$_3$	ICM-103-2NH$_3$-1	ICM-103-2NH$_3$-2	
HS				
$E\%$	83	76	71	
	ICM-103-4H$_2$S	ICM-103-2H$_2$S-1	ICM-103-2H$_2$S-2	
HS				
$E\%$	83	6%	66	

Fig. 5 Fingerprint plots for ten ICM-103 crystals. The points on the plot with no contribution on the surface are uncolored, and points with a contribution to the surface are colored blue for a small contribution through blue-green to green for a higher contribution.

the stabilization effect of small molecules is also related to the energetic molecule. Finally, the number and position of small molecules also affect close contact. In each series, the crystals with four small molecules have stronger close contacts than crystals with two. In addition, it is found that ICM-103-2H₂O-2 has stronger close contacts than ICM-103-2H₂O-1, while this is just

the opposite for ICM-103-2NH$_3$-1 and ICM-103-2NH$_3$-2. The difference in close contacts between ICM-103-2H$_2$S-1 and ICM-103-2H$_2$S-2 is not obvious. This shows that the effect of the position on close contacts is coupled with the type of small molecules.

Table 3 lists the calculated stabilization energy (ΔE) for nine crystals with small molecules. It is seen that all of them have
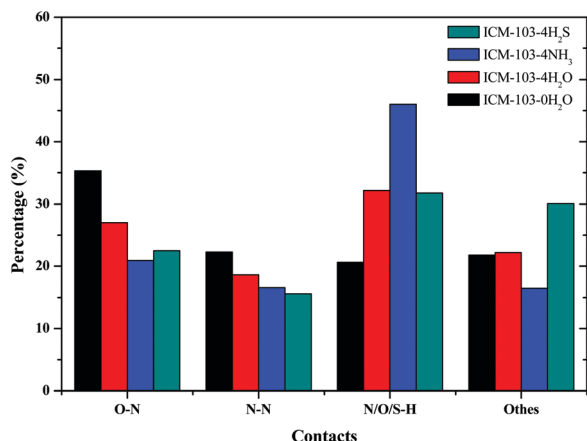
Fig. 6 The percentage of main close contacts in four ICM-103 crystals.

negative ΔE values, showing that the H_2O, NH_3, and H_2S can decrease the total energy and stabilize the whole ICM-103 crystal. ICM-103-$4H_2O$ has a negative ΔE value than ICM-103-$2H_2O$-1 and ICM-103-$2H_2O$-2, and this is true for NH_3-crystals and H_2S-crystals. Besides, it is interesting to find the ΔE value of ICM-103-$4H_2O$ is even lower than the sum of ICM-103-$2H_2O$-1 and ICM-103-$2H_2O$-2, indicating that the two H_2O molecules in position 1 and position 2 may have synergy to stabilize the system in ICM-103-$4H_2O$, and this is also true for ICM-103-$4NH_3$ and ICM-103-$4H_2S$, showing that the stabilization effect on crystals of small molecules can be further strengthened with the increasing number. But the effect of the position on ΔE is controlled by the type of small molecules, and the ΔE of ICM-103-$2H_2O$-2 is 0.2 eV lower than ICM-103-$2H_2O$-1, while ICM-103-$2NH_3$-1 has negative ΔE than ICM-103-$2NH_3$-2, ICM-103-$2H_2S$-1, and ICM-103-$2H_2S$-2 have the same ΔE, showing that the two H_2O molecules in position 2 are more helpful for stabilizing the ICM-103 crystal, while for NH_3, it is position 1. The result obtained by stabilization energy is in agreement with those by Hirshfeld surface and fingerprint plots. In all, three small molecules can stabilize the ICM-103 crystal and increase in the order of H_2S, H_2O, and NH_3. This effect is further enhanced with the increment of the number by the synergy between small molecules in positions 1 and 2.

3.4. Optical properties

Light is also one kind of energy and stimulus, and many energetic crystals are sensitive to light and respond to its stimulus differently. Therefore, important optical properties, including the absorption spectra, dielectric function, and refractive index of ICM-103 crystals, were studied in this section, and the effects of the number of H_2O, NH_3 and H_2S in positions 1 and 2 were also investigated. Firstly, absorption coefficient $\alpha(\omega)$ was calculated by the equation:[27] $\alpha(\omega) = \sqrt{2}\left[\sqrt{\varepsilon_1^2 + \varepsilon_2^2} - \varepsilon_1\right]^{\frac{1}{2}}$ (ε_1 and ε_2 are the real part and imaginary part of the dielectric function, respectively), as it is a common

parameter used to estimate the absorption intensity under different wavelengths of light. Fig. 8 depicts the predicted absorption spectra of ten ICM-103 crystals. First, it is found that the absorption spectra of ICM-103-$2H_2O$-1 and ICM-103-$2H_2O$-2 are almost the same, making their absorption spectra overlap each other in Fig. 8. This is also true for ICM-103-$2H_2S$-1 and ICM-103-$2H_2S$-2, showing that the position of H_2S and H_2O affect the absorption spectra. But this is not true for NH_3-crystals, as seen from Fig. 8 that the absorption intensity of ICM-103-$2NH_3$-2 is obviously stronger than that of ICM-103-$2NH_3$-1 to light in the range of 200–600 nm. Then, it can be seen that different types and numbers of small molecules have different effects on the absorption spectra at a different wavelength range of light. For H_2O-crystals, three peaks occur at around 320 nm (strongest), 135 nm and 85 nm, which are located in the ultraviolet region. The difference in the position of the peak is small, but and the absorption coefficient decreases with the order of ICM-103-$0H_2O$, ICM-103-$2H_2O$-1/2 and ICM-103-$4H_2O$ in this region (10–400 nm), showing that H_2O will reduce the absorption intensity to ultraviolet light, and this is also true for NH_3 and H_2S. While this order is just the opposite to the light with a longer wavelength (>400 nm), indicating that H_2O can enhance the absorption to visible light and infrared light, which is also true for NH_3. For NH_3-crystals, the number and position of main adsorption peaks are similar to those of H_2O-crystals, but the absorption intensity and order for the three NH_3-crystals are obviously different from those of H_2O-crystals. Generally, the absorption coefficient decreases in the order of ICM-103-$2NH_3$-2, ICM-103-$2NH_3$-1, and ICM-103-$4NH_3$ in the region of 10–400 nm, but the order is ICM-103-$4NH_3$, ICM-103-$2NH_3$-2, and ICM-103-$2NH_3$-1 in the 400–750 nm region, and ICM-103-$2NH_3$-1, ICM-103-$4NH_3$ and ICM-103-$2NH_3$-2 in the 750–1200 nm region, respectively. This shows that two NH_3 in position 2, four NH_3, and two NH_3 in position 1 are more favourable for absorbing ultraviolet light, visible light, and infrared light, respectively. Finally, different from H_2O and NH_3, three peaks at around 300 nm, 125 nm, and 82 nm in the absorption spectra for H_2S-crystals indicate the blue-shift. The difference in absorption spectra for three H_2S-crystals is negligible, showing that the number and position of H_2S almost have no effects on the absorption to different wavelengths. In all, small molecules H_2O, NH_3, and H_2S influence the $\alpha(\omega)$ and absorption strength to different wavelengths of light, and effects are also related to their number and position.

Fig. 9 displays the real part ε_1 and imaginary part ε_2 of the dielectric function of ten ICM-103 crystals. The whole shape and changing trend of the dielectric function for ten crystals are similar to some degree, but differences caused by the small molecules have been observed and cannot be neglected. Previous works have used the first principle method to predict the dielectric constant $\varepsilon_1(0)$ of several energetic compounds (like AP and NaN_3) and found that the theoretical values are in agreement with the experimental results.[28,29] As seen from Fig. 9 and Table 3, first, the $\varepsilon_1(0)$ value of all ICM-103-$0H_2O$ crystal is 1.941, showing its small electron binding ability and
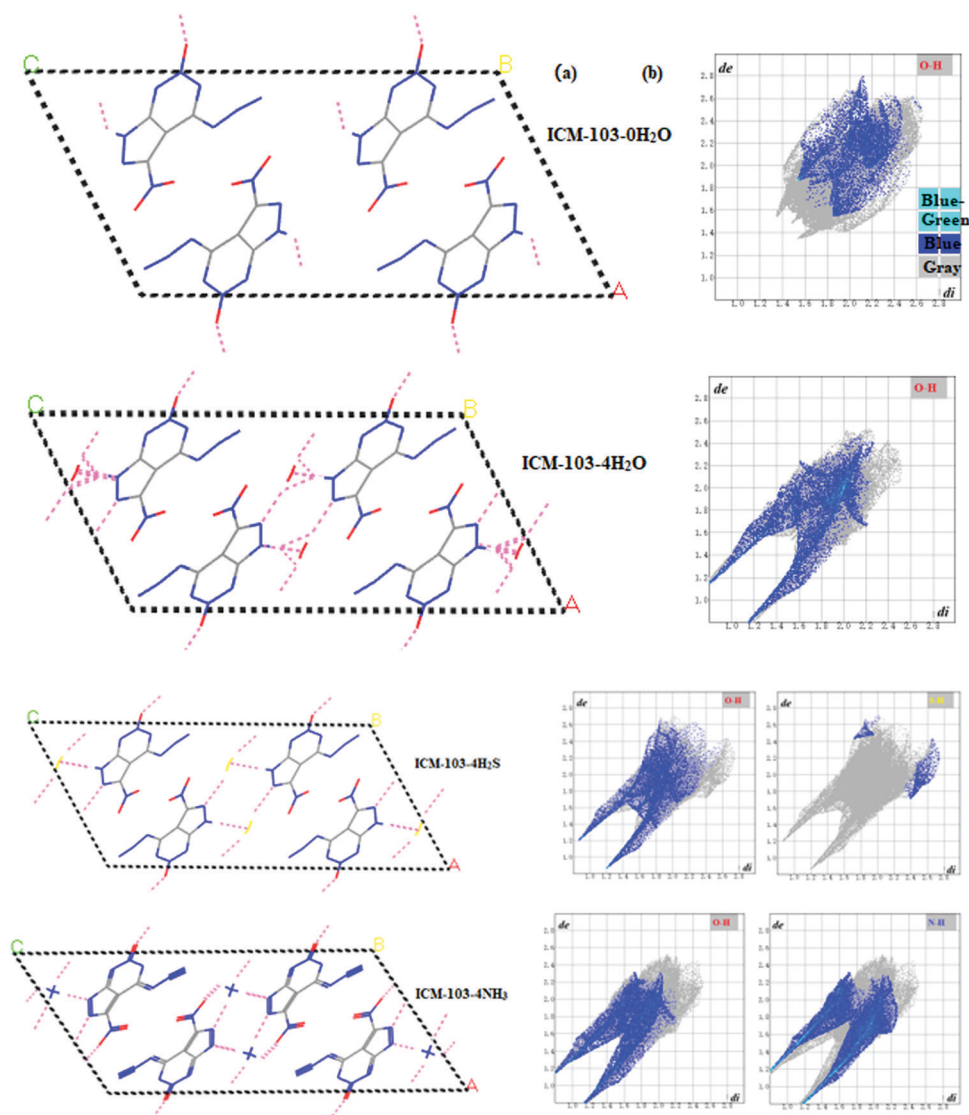
Fig. 7 The intermolecular contact network (dash line) and fingerprint plots for N/O/S···H contacts in four ICM-103 crystals. The points on the plot with no contribution on the surface are uncolored and colored gray, and points with a contribution to the surface are colored blue for a small contribution to blue-green for a big contribution.

electric polarization ability. But this can be slightly increased by three small molecules, as the other nine crystals all have higher $\varepsilon_1(0)$ than ICM-103-0H$_2$O. For the crystals with four small molecules, $\varepsilon_1(0)$ decreases in the order of ICM-103-4H$_2$O, ICM-103-4NH$_3$, and ICM-103-4H$_2$S. But this is different for crystals with two small molecules, and $\varepsilon_1(0)$ decreases in the order of ICM-103-2NH$_3$-1/2, ICM-103-2H$_2$S-1/2, and ICM-103-2H$_2$O-1/2. The position also has effects on $\varepsilon_1(0)$ and is related to the type of small molecules. For example, $\varepsilon_1(0)$ values for ICM-103-2H$_2$O-1 and ICM-103-2H$_2$O-2 are the same, and this is also true for ICM-103-2H$_2$S-1 and ICM-103-2H$_2$S-2, and their values are both lower than the corresponding crystal with four small molecules, respectively. But ICM-103-2NH$_3$-2 has higher $\varepsilon_1(0)$ than ICM-103-2NH$_3$-1, which in turn is higher than ICM-103-4NH$_3$. Generally, the $\varepsilon_1(0)$ values of ten ICM-103 crystals are between the value of energetic compounds AP

and metal-azides, which conforms to the characteristic of energetic crystals. Then, ε_1 of ICM-103-0H$_2$O reaches the three largest peak values at the energy of 2.85 eV (the strongest peak), 9.51 eV (weak peak), and 14.33 eV (weak peak). But these three peaks will shift to lower energy in general due to the existence of small molecules, especially for the NH$_3$-crystals, and the strongest peak of its three related crystals occur at energies 1.72 eV (ICM-103-4NH$_3$), 1.62 eV (ICM-103-2NH$_3$-1), and 2.19 eV (ICM-103-2NH$_3$-2), respectively. The ε_1 within the 4.24–5.06 eV of ICM-103-0H$_2$O is lower than zero, indicating that light cannot be transmitted in its solid crystals in this region. This is similar for ICM-103-2H$_2$O-1 and ICM-103-2H$_2$O-2, ICM-103-4H$_2$S, ICM-103-2H$_2$S-1 and ICM-103-2H$_2$S-2. But this region is changed to 3.96–4.79 eV and 4.06–4.72 eV, respectively. While for ICM-103-4NH$_3$ and ICM-103-2NH$_3$-1, the ε_1 values are all positive, and this untransmittable region is eliminated completely.
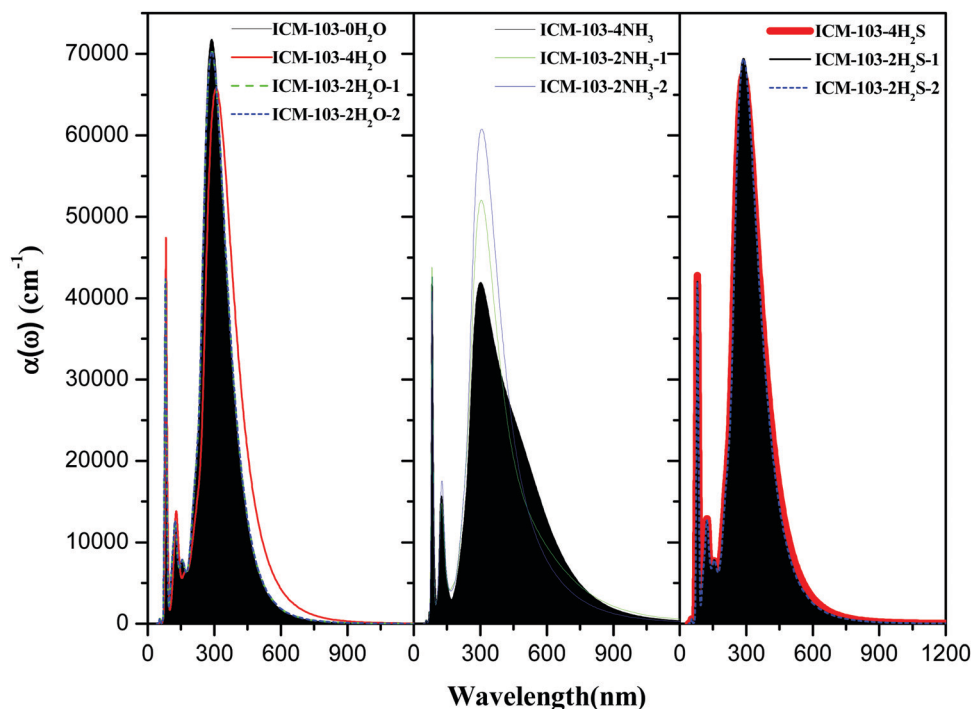
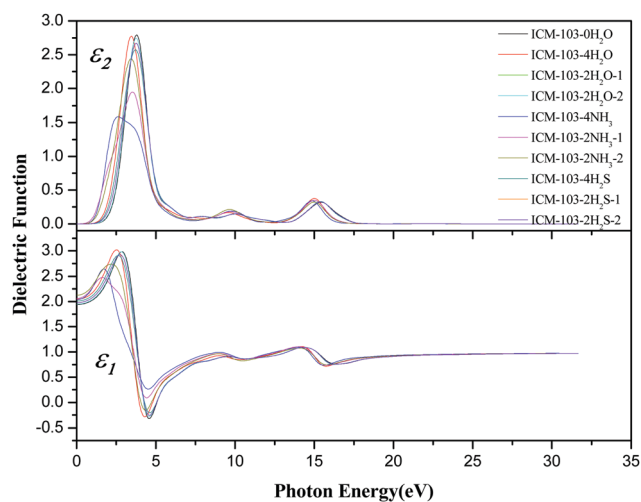**Fig. 8** The predicted absorption spectra of ten ICM-103 crystals.

Fig. 9 The predicted dielectric function of ten ICM-103 crystals.

Then, the imaginary part ε_2 can reflect the information of electron transition, as seen from Fig. 9. For ICM-103-0H$_2$O, it increases gradually from 0 eV and peaks at 3.78 eV with the strongest intensity, and another two weak peaks occur at 10.02 eV and 15.43 eV. The first strong peak is due to the electron transition mainly from the high valence band into the low conduction band, while the rest are caused by transmitting other different valence electrons into the conduction band. The shapes of ε_2 for the other nine crystals are similar to ICM-103-0H$_2$O, and the position and intensity of peaks are different to some degree. For instance, the position of the first

peak is shifted to lower energy with lower intensity for all nine crystals compared to ICM-103-0H$_2$O, which is consistent with the fact that their band gap values are lower than ICM-103-0H$_2$O. The ε_2 of NH$_3$-crystals at low energy (<2.5 eV) is higher than other crystals, showing that NH$_3$-crystals can adsorb more photons in the long wavelength region like infrared and visible light, which is in agreement with the results of absorption spectra. Finally, the refractive index (n) and extinction coefficient (k) are obtained by these two equations: $\varepsilon_1 = n^2 - k^2$ and $\varepsilon_2 = 2nk$, as depicted in Fig. 10. The theoretical static refractive index n_0 ($n_0 = \sqrt{\varepsilon_1(0)}$) values of ten ICM-103 crystals are listed in Table 3. The n_0 value increases in the order of
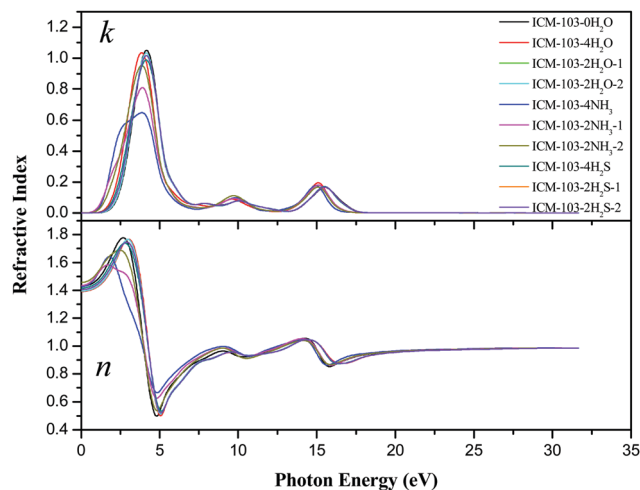

Fig. 10 The predicted refractive index of ten ICM-103 crystals.

ICM-103-0H$_2$O, ICM-103-2H$_2$O-1/2, ICM-103-2H$_2$S-1/2, ICM-103-4H$_2$S, ICM-103-4NH$_3$, ICM-103-4H$_2$O, ICM-103-2NH$_3$-1, and ICM-103-2NH$_3$-2, showing that the three small molecules can enhance the ability to refract light and increases in the order of H$_2$S, H$_2$O, and NH$_3$ in general, and the position and number of molecules also has an influence. Then, the shapes and changing trends of n and k for each ICM-103 crystal are similar to those of ε_1 and ε_2, respectively. The energy regions within $k > n$ for some crystals correspond to those of $\varepsilon_1 < 0$. In all, these results show that the type, number, and position of three small molecules do have a significant effect on the optical properties of ICM-103 crystals.

4. Conclusions

In this work, the functions of three molecules H$_2$O, NH$_3$, and H$_2$S on stabilizing the crystal structure of the high energy compound ICM-103 were investigated using the first principle calculation and Hirshfeld surface analysis. The effects of type, number, and position on the molecular, crystal and electronic structures, safety and optical properties were also studied. The results show that H$_2$O, NH$_3$, and H$_2$S can stabilize the crystal structure and have different effects on the structure and properties. (1) They change the lattice parameter of ICM-103 crystals and shorten the bond length of weak C–NO$_2$ bonds and N–N bonds in the N$_3$ group. (2) The NH$_3$ transforms the crystal from neutral to ionic type energetic compounds by the hydrogen transition from the ICM-103 molecule to NH$_3$. (3) They all contribute to DOS at different energy regions and generate new energy levels in the band structure. The number and position of these molecules also have different effects on the electronic structure, especially in the case of NH$_3$. (4) The low band gap, relative high $E\%$ value, and low percentage of hydrogen bonding in close contacts show the sensitive feature of ICM-103, which is used as initiating explosives. (5) H$_2$O, NH$_3$, and H$_2$S can stabilize the crystal structure of ICM-103 and reduce the sensitivity by increasing the $E\%$ value, enhancing and enriching the close contacts, especially the hydrogen-bonding contact. (6) The stabilization energy of crystals with four small molecules is obviously higher than the sum of the corresponding two crystals with two small molecules, showing that the small molecules in the two positions can cooperate with each other to better stabilize the crystal structure. (7) This stabilization effect increases in the order of H$_2$S, H$_2$O and NH$_3$, and the NH$_3$ in position 1 is more favorable for stabilizing the crystal structure than that in position 2, but the position of H$_2$S and H$_2$O almost has a negligible effect. (8) H$_2$O and NH$_3$ reduce the absorption intensity to ultraviolet light but enhance the absorption to visible light and infrared light, and the number and position of H$_2$S almost have no effects on the absorption to light of different wavelengths. (9) They all increase the dielectric constant and static refractive index in the order of H$_2$S, and H$_2$O, NH$_3$. NH$_3$ can eliminate the region in which the light cannot be transmitted in H$_2$O-crystals, H$_2$S-crystals, and ICM-103-0H$_2$O. This work may be helpful for understanding the stabilizing effect of small molecules on unstable high energy crystals. Since H$_2$O, NH$_3$, and H$_2$S are non-energy or low-energy molecules whose presence will harm the energy performance of high energy compounds, studies on searching for new small molecules with higher energy to stabilize and adjust the unstable energetic crystal system may be needed.

Conflicts of interest

The authors declare no conflicts of interest.

Acknowledgements

References

1 Y. G. Xu, Q. Wang, C. Shen, Q. H. Lin, P. C. Wang and M. Lu, A series of energetic metal pentazolate hydrates, *Nature*, 2017, **549**, 78–81.

2 C. Zhang, C. G. Sun, B. C. Hu, C. M. Yu and M. Lu, Synthesis and characterization of the pentazolate anion cyclo-N$_5^-$ in (N$_5$)$_6$(H$_3$O)$_3$(NH$_4$)$_4$Cl, *Science*, 2017, **355**(6323), 374–376.

3 Y. G. Xu, P. C. Wang, Q. H. Lin, X. F. Mei and M. Lu, Self-assembled energetic 3D metal–organic framework [Na$_8$(N$_5$)$_8$(H$_2$O)$_3$]$_n$ based on cyclo-N$_5^-$, *Dalton Trans.*, 2018, **7**(45), 1398–1401.

4 Y. C. Li, K. C. Wang, S. W. Song, X. J. Qi, W. Q. Zhang, M. C. Deng and Q. H. Zhang, [LiNa(N$_5$)$_2$(H$_2$O)$_4$]·H$_2$O: a novel heterometallic cyclo-N$_5^-$framework with helical chains, *Sci. China Mater.*, 2019, **62**(02), 283–288.

5 Y. G. Xu, Q. H. Lin, P. C. Wang and M. Lu, Syntheses, crystal structures and properties of a series of 3D metal–inorganic frameworks containing pentazolate anion, *Chem. – Asian J.*, 2018, **13**(13), 1669–1673.

6 Y. G. Xu, L. L. Tian, D. X. Li, P. C. Wang and M. Lu, A series of energetic cyclo-pentazolate salts: rapid synthesis, characterization, and promising performance, *J. Mater. Chem. A*, 2019, **7**(20), 12468–12479.

7 Y. G. Xu, L. J. Ding, F. Yang, D. X. Li, P. C. Wang, Q. H. Lin and M. Lu, LiN$_5$: a novel pentazolate salt with high nitrogen content, *Chem. Eng. J.*, 2022, **429**, 132399.

8 W. Q. Zhang, J. H. Zhang, M. C. Deng, X. J. Qi, F. D. Nie and Q. H. Zhang, A promising high-energy-density material, *Nat. Commun.*, 2017, **8**(1), 181.

9 Y. Wang, Y. J. Liu, S. W. Song, Z. J. Yang, X. J. Qi, K. C. Wang, Y. Liu, Q. H. Zhang and Y. Tian, Accelerating the discovery of insensitive high-energy-density materials by a materials genome approach, *Nat. Commun.*, 2018, **9**(1), 2444.

10 M. C. Deng, Y. G. Feng, W. Q. Zhang, X. J. Qi and Q. H. Zhang, A green metal-free fused-ring initiating substance, *Nat. Commun.*, 2019, **10**(1), 1339.

11 B. C. Tappan and T. B. Brill, Thermal decomposition of energetic materials 86. cryogel synthesis of nanocrystalline CL-20 coated with cured nitrocellulose, *Propellants, Explos., Pyrotech.*, 2003, **28**(5), 223–230.

12 J. H. Luo, L. Y. Chen, D. N. Nguyen, D. Guo, Q. An and M. J. Cheng, Dual functions of water in stabilizing metal-pentazolate hydrates $[M(N_5)_2(H_2O)_4]\cdot 4H_2O$ (M = Mn, Fe, Co, and Zn) high-energy-density materials, *J. Phys. Chem. C*, 2018, **122**(37), 21192–21201.

13 C. J. Wu, L. E. Fried, L. H. Yang, N. Goldman and S. Bastea, Catalytic behaviour of dense hot water, *Nat. Chem.*, 2009, **1**(1), 57–62.

14 Q. Wu, W. H. Zhu and H. M. Xiao, Catalytic behavior of hydrogen radicals in the thermal decomposition of crystalline furoxan DFT-based molecular dynamics simulations, *RSC Adv.*, 2014, **4**(65), 34454–34459.

15 T. Zeng, R. J. Yang, D. H. Li, J. M. Li, X. Y. Guo and P. Luo, Reactive molecular dynamics study on the effect of H_2O on the thermal decomposition of ammonium dinitramide, *Propellants, Explos., Pyrotech.*, 2020, **45**(10), 1590–1599.

16 Q. Wu, M. Q. Li, Q. N. Hu, Z. W. Zhang and W. H. Zhu, First principle study and Hirshfeld surface analysis on the effect of H2O, NH3 and H2S on structural, electronic, elastic, optical and thermodynamic properties of a novel high energy crystal 2,4,6-triamino-5-nitropyrimidine-1,3-dioxide, *J. Mater. Sci.*, 2020, **55**(1), 237–249.

17 R. Matyáš and J. Pachman, *Primary Explosives*, Springer Berlin Heidelberg, 2013, ch. 6.

18 D. Fischer, T. M. Klapötke and J. Stierstorfer, Potassium 1,1′-dinitramino-5,5′-bistetrazolate: a primary explosive with fast detonation and high initiation power, *Angew. Chem., Int. Ed.*, 2014, **53**(31), 8172–8175.

19 S. J. Clark, M. D. Segall, C. J. Pickard, P. J. Hasnip, M. I. Probert, K. Refson and M. C. Payne, First principles methods using CASTEP, *Z. Kristallogr.*, 2005, **220**, 567–570.

20 D. R. Hamann, M. Schlüter and C. Chiang, Norm-conserving pseudopotentials, *Phys. Rev. Lett.*, 1979, **43**(20), 1494.

21 F. Ortmann, F. Bechstedt and W. G. Schmidt, Semiempirical van der Waals correction to the density functional description of solids and molecular structures, *Phys. Rev. B: Condens. Matter Mater. Phys.*, 2006, **73**, 205101.

22 T. H. Fischer and J. Almlof, General methods for geometry and wave function optimization, *J. Phys. Chem.*, 1992, **96**(24), 9768–9774.

23 S. Wolff, D. Grimwood, J. McKinnon, M. Turner, D. Jayatilaka and M. Spackman, *Crystalexplorer (version 3.0)*, University of Western Australia, 2012.

24 W. Q. Zhang, J. H. Zhang, M. C. Deng, X. J. Qi, F. D. Nie and Q. H. Zhang, A promising high-energy-density material, *Nat. Commun.*, 2017, **8**, 181.

25 B. B. Tian, Y. Xiong, L. Z. Chen and C. Y. Zhang, Relationship between the crystal packing and impact sensitivity of energetic materials, *CrystEngComm*, 2018, **20**(6), 837–848.

26 Y. Ma, L. Y. Meng, H. Z. Li and C. Y. Zhang, Enhancing intermolecular interactions and their anisotropy to build low-impact-sensitivity energetic crystals, *CrystEngComm*, 2017, **19**(23), 3145–3155.

27 S. Saha and T. P. Sinha, Electronic structure, chemical bonding, and optical properties of paraelectric $BaTiO_3$, *Phys. Rev. B: Condens. Matter Mater. Phys.*, 2000, **62**(13), 8828.

28 W. H. Zhu, J. J. Xiao and H. M. Xiao, Comparative first-principles study of structural and optical properties of alkali metal azides, *J. Phys. Chem. B*, 2006, **110**(20), 9856–9862.

29 B. Liu, X. J. Wang, X. Y. Bu and X. Yao, Study on First principles of Optical Properties of NH_4ClO_4, *Chinese, J. Energ. Mater.*, 2015, **23**(10), 1024–1027.